J Mater Sci (2008) 43:510–524
DOI 10.1007/s10853-007-1849-6

5TH BRAZILIAN MRS MEETING

Morphological, mechanical, and biocompatibility characterization of macroporous alumina scaffolds coated with calcium phosphate/PVA

Hermes S. Costa · Alexandra A. P. Mansur · Edel F. Barbosa-Stancioli · Marivalda M. Pereira · Herman S. Mansur

Received: 29 December 2006 / Accepted: 14 May 2007 / Published online: 20 July 2007

Abstract In bone tissue engineering, a highly porous artificial extracellular matrix or scaffold is required to accommodate cells and guide the tissue regeneration in three-dimension. Calcium phosphate (CaP) ceramics are widely used for bone substitution and repair due to their biocompatibility, bioactivity, and osteoconduction. However, compared to alumina ceramics, either in the dense or porous form, the mechanical strength achieved for calcium phosphates is generally lower. In the present work, the major goal was to develop a tri-dimensional macroporous alumina scaffold with a biocompatible PVA/calcium phosphate coating to be potentially used as bone tissue substitute. This approach aims to combine the high mechanical strength of the alumina scaffold with the biocompatibility of calcium phosphate based materials. Hence, the porous alumina scaffolds were produced by the polymer foam replication procedure. Then, these scaffolds were submitted to two different coating methods: the biomimetic and the immersion in a calcium phosphate/polyvinyl alcohol (CaP/PVA) slurry. The microstructure, morphology and crystallinity of the macroporous alumina scaffolds samples and coated with CaP/PVA were characterized by X-ray diffraction (XRD), Fourier Transform Infrared Spectroscopy (FTIR) and Scanning Electron Microscopy (SEM/EDX) analysis. Also, specific surface area was assessed by BET nitrogen adsorption method and mechanical behavior was evaluated by axial compression tests. Finally, biocompatibility and cytotoxicity were evaluated by VERO cell spreading and attachment assays under SEM. The morphological analysis obtained from SEM photomicrograph results has indicated that 3D macroporous alumina scaffolds were successfully produced, with estimated porosity of over 65% in a highly interconnected network. In addition, the mechanical test results have indicated that porous alumina scaffolds with ultimate compressive strength of over 3.0 MPa were produced. Concerning to the calcium phosphate coatings, the results have showed that the biomimetic method was not efficient on producing a detectable layer onto the alumina scaffolds. On the other hand, a uniform and adherent inorganic–organic coating was effectively formed onto alumina macroporous scaffold by the immersion of the porous structure into the CaP/PVA suspension. Viable VERO cells were verified onto the surface of alumina porous scaffold samples coated with PVA–calcium phosphate. In conclusion, a new method was developed to produce alumina with tri-dimensional porous structure and uniformly covered with a biocompatible coating of calcium phosphate/PVA. Such system has high potential to be used in bone tissue engineering.

H. S. Costa · A. A. P. Mansur · M. M. Pereira · H. S. Mansur (✉)
Laboratory of Biomaterials and Tissue Engineering, Department of Metallurgical and Materials Engineering, Federal University of Minas Gerais, R. Espírito Santo 35, Belo Horizonte, MG, Brazil
e-mail: hmansur@demet.ufmg.br

E. F. Barbosa-Stancioli
Department of Microbiology, Institute of Biological Sciences, Federal University of Minas Gerais, PO Box 486, 31270 901 Belo Horizonte, MG, Brazil

Introduction

Hard tissue diseases and defects, osteoporosis, and osteoarthritis are some of the most significant related medical conditions leading to an extensive need for the use of appropriate implant materials [1]. In the field of dental

surgery, some applications of biomaterials include filling of pockets and maxillary ridge augmentation, deficiencies caused by loss of dentition with advancing age or various diseases [2]. Natural bone is a porous tissue that consists of a solid matrix containing voids of varying sizes. It is a specialized connective tissue consisting of collagen, mineral, and water arranged in a specific spatial distribution [3]. Materials alternatives to substitute or regenerate bone tissue are autographs, allographs, or artificial materials. Compared to traditional autograph and allograph procedures, use of synthetic materials eliminates problems of donor scarcity, supply limitation, pathogen transfer, and immune rejection.

Different approaches applying synthetic materials are in current utilization to solve bone tissue related clinical conditions. One of them is the use of porous materials as bone substitute [4]. When pore sizes exceed 100 μm, bone will grow within the interconnecting pore channels near the surface and maintain its vascularity and long-term viability. In this manner, the implant serves as a structural bridge or scaffold for bone formation. The advantage offered by porous implant is the mechanical stability developed when bone grows into the pores of the material. Mechanical requirements of prosthesis, however, severely restrict the use of low-strength porous implants to low-load or non-load bearing applications [5]. Consequently, synthetic 3D porous scaffolds have potential application on bone regeneration in minor osseous defects, for instance localized tissue losses and atrophies to be used as tissue substitutes in the field of dentistry and orthopedics cancellous bone. On the other hand, in severe trauma cases, in the correction of large bone tissue defects, where a significant part of the bone is missing or damaged, dense ceramic implants such as alumina or ZTA (ZTA—zirconia toughened alumina) are used to replace or augment the missing or fractured bone [6].

Several porous materials produced by different synthesis methods [7, 8] have been developed and used as bone implants such as corals derivatives, calcium phosphates, alumina, titania, polyurethane, Co–Cr alloys, PMMA, with the calcium phosphates being the most acceptable. Calcium phosphate ceramics have been extensively used as a material for bone substitution and repair, due to its biocompatibility, bioactivity and osteoconduction [9]. However, compared to alumina ceramics, either in the dense or porous form, the mechanical strength achieved for calcium phosphates are generally lower [10–12]. Moreover, it has been recently [13] demonstrated that using zinc (Zn^{2+}) associated with calcium phosphates has enhanced the bioactivity in bone tissue regeneration. Other role of zinc is protecting biological structures from damage by free radicals. It is worth to be mentioned that zinc must be released slowly from the implant because zinc at an elevated level induces adverse reactions.

The objective of this work is the production of a porous bioceramic for potential use as bone substitute, in which a porous alumina scaffold, with high interconnectivity, is coated with a calcium phosphate layer. This approach aims to combine the higher strength of the alumina scaffold with the biological advantages of the calcium phosphate surface, that is, its bioactivity and osteoconduction properties.

Materials and methods

Materials

The selection of ceramic powder material for this work was based in two premises: (i) use of a high purity alumina, fine grained in the submicron size range and standard for alumina-based bioceramics; (ii) use of material produced by a local company to guarantee availability and relatively low cost. Hence, two alumina powders were used in the experiments: (i) a commercial alumina powder from Vetec Química Fina Ltda, Brazil (sample A-01): (ii) alumina powder (sample A-02) supplied by Sigma-Aldrich, product catalog #544833, and named as nanosized alumina powder.

The commercial alumina sample A-01 (local company) was supplied as coarser powder and, for that reason, was not readily adequate for the production of a stable and fine particle size suspension due to the broad distribution of particle size and large average size. Therefore, we have used particle milling (US Stoneware, jar diameter φ = 130 mm) without optimizing the operational parameter conditions, focused on reducing particle size but not specifically on the efficiency of the process itself. It took 48 h to obtain some significant particle size reduction.

In order to investigate the particle size distribution, morphology, and specific surface area of alumina samples several characterization techniques were used. Particle size distribution analysis was obtained by laser scattering using CILAS model 1064 (range 500–0.1 μm). Scanning electron microscopy (SEM, model JEOL JSM-6360LV, EDX, Thermo Noran) was also used for particle morphology and size evaluation. Surface area of alumina powders was characterized by multipoint B.E.T. (Brunauer, Emmett, and Teller) nitrogen adsorption method (QUANTACHROME, NOVA®-1200 V.5.25), with minimum 8 h of degassing at 110 °C. Ceramic powder crystallinity was assessed by X-ray diffraction (XRD) analysis (PHILIPS, model PW1710, KαCu λ = 1.54060 Å). Chemical analysis of alumina powders (A-01 and A-02) was conducted by X-ray fluorescence (XRF, PHILIPS, model PW 9710). The chemical characteristics of all powders, dispersants, and binders were analyzed by IR absorption spectra, which were obtained by using diffuse reflectance infrared Fourier transform spectrometry (DRIFTS) (Perkin-Elmer, Paragon

1000). Powder samples were dispersed with pre-dried KBr (110 °C, 2 h, spectroscopy grade, Sigma) with a weight ratio of 1:10 for measurements.

Alumina scaffolds production

Preparation of alumina suspensions

Alumina suspensions were prepared using polyvinyl alcohol (PVA) as binder with hydrolysis grade 98.0–98.8% and molecular weight 31,000 and 50,000 g/mol (Celvol 107—Celanese Chemicals). PVA solutions with concentration 10.0 wt% were prepared by dissolving PVA granules in deionized water at 90 °C for 30 min.

To establish a comparative study, two types of dispersants were used. The first one consisted of Polyacrylic acid (PAA) with average molecular weight of 250,000 g/mol (Aldrich). The other one was Polyvinyl pyrrolidone (PVP) with molecular weight 40,000 g/mol (Vetec, Brazil).

Three different routes were used for the preparation of the alumina suspensions for the fabrication of scaffolds. In the two first routes (R1 and R2), suspensions of the alumina powder A-01 were prepared in a mixture of 70% ethanol and 30% water. In the first route (R1), PVP was added as dispersant to the alumina suspension and was thoroughly stirred for 2 h. Then, PVA was added and the suspension stirred for another 15 min. The second route (R2) utilized PAA as major dispersant was added to the alumina suspension and vigorously stirred for 2 h. In the sequence, PVP and PVA additives were added to the suspension, and the mixture was kept under agitation for another 15 min. Then, the suspension was left resting for a 24-h period reaching a better surface adsorption of the additives onto the alumina particles. In the third route (R3), alumina nanosized particles (A-02) were use to prepare the suspensions and a stirring procedure similar to R1 was utilized. Table 1 summarizes the concentrations of additives used in the different preparation routes. The concentration of additives was determined based on the dry weight of alumina powder. All suspensions were prepared at room temperature (25 ± 2 °C) using double distilled water.

Suspension sedimentation tests

Sedimentation experiments were carried out under various conditions to determine the amount of dispersants, and effect of pulp density on the stability of dispersion aiming to obtain a uniform coating on the polyurethane porous template. Previously prepared alumina suspension samples produced by the three routes were then transferred to a 50 mL graduated cylinder, where the sedimentation tests have taken place. A blank sedimentation test without any dispersant was also investigated and used as reference.

Polymer foam replication

The alumina porous body was fabricated by immersing the struts of polyurethane (PU) foam (50 pores per inch-ppi) in alumina slurry. PU samples were cut to cubic blocks with average dimensions of $10 \times 10 \times 10$ mm^3. Polyurethane blocks were immersed in the previously prepared alumina suspensions, slightly pressed three times to remove air and allowing a better penetration of the suspension into the foam pore structure. The PU guide porous structures were removed from alumina suspension and a final squeeze was performed to remove the entrapped excess of suspension. Then, they were partially dried for 5 min at 80 °C and slightly pressed again to remove the excess of suspension. The procedure of immersion and drying of the PU foams to fabricate alumina coating was repeated for three cycles. The samples were dried at 80 °C for 24 h and fired in a furnace using a heating rate of 3 °C/min up to 600 °C, to enable complete burnout of the organic components. Subsequently, samples were heated up to the sintering temperature of 1,550 °C and maintained for 3 h. Finally, the prepared macroporous alumina bodies were cooled to room temperature.

Alumina scaffolds coating methods

In order to obtain a bioactive surface on the previously produced macroporous alumina scaffolds, two different coating methods were tested. The first was the biomimetic

Table 1 Compositions of the alumina suspensions

Sample route	Solvent ethanol/water (% v/v)	Powder Al_2O_3 (% p/v)	Dispersant PAA (% p/v)	Dispersant PVP (% p/v)	Binder PVA (% p/v)
R1	70/30	15 (A-01)	–	0.5	3.0
		25 (A-01)	–	0.5	3.0
R2	70/30	15 (A-01)	1.5	0.5	3.0
		25 (A-01)	0.9	0.5	3.0
R3	70/30	15 (A-02)	–	0.5	3.0
		25 (A-02)	–	0.5	3.0

coating method, in which samples were immersed in simulated body fluid (SBF) with pH = 7.40 and ionic composition ($[Na^+]$ = 142.0, $[K^+]$ = 5.0, $[Ca^{2+}]$ = 2.5, $[Mg^{2+}]$ = 1.5, $[Cl^-]$ = 147.8, $[HCO_3^-]$ = 4.2, $[HPO_4^{2-}]$ = 1.0, $[SO_4^{2-}]$ = 0.5, mmol/dm^3) equal to those in blood plasma. Samples were soaked in SBF for 7 days at (36 ± 1) °C, and after that period, the original SBF solution was substituted twice for a new solution with 40% higher ion concentration (1.4 SBF). Then, the immersion procedure of alumina samples was maintained for a week, each time, leading to a total period of 21 days. Samples were than removed, slightly rinsed in distilled water and dried at room temperature. Control samples were kept immersed in deionized water for the same 21 days.

The second coating method was the immersion of the porous alumina scaffold in the aqueous/alcoholic slurry of calcium phosphate/PVA. The synthesis of the CaP followed the procedure previously reported by our group [14, 15]. The CaP powder was used in the dried condition, with particle size below 400 mesh (<38 μm). Calcium phosphate powder was added to the formerly prepared PVA solution with final ratio of PVA:CaP = [1:1]. Macroporous alumina scaffold samples were immersed in the suspension and maintained under moderate stirring for 60 min. Finally, samples were removed from the CaP/PVA suspension and dried at room temperature for 24 h.

A solution of $Zn(NO_3)_2{\cdot}6H_2O$ with concentration of 1.0 wt% in aqueous/ethanol (70/30 vol%) was prepared and alumina scaffolds with calcium phosphate coating were immersed for 30 min for Zn^{2+} incorporation under moderate magnetic stirring.

Alumina scaffolds characterization

Scanning electron microscopy (SEM) was used for evaluating the morphology and structure of produced 3D macroporous alumina scaffolds and CaP/PVA coatings. Alumina spongy samples phases and crystallinity after thermal treatment were assessed by X-ray diffraction (XRD) analysis. Also, calcium phosphate powder samples and CaP with Zn^{2+} incorporated to the ceramic matrix were also investigated by XRD. The chemical characteristics of powders, polymers (dispersants and binders), and alumina coated scaffolds after comminution were analyzed by FTIR absorption spectroscopy within the range between 4,000 and 400 cm^{-1}, by using diffuse reflectance method. Powder samples were mixed with pre-dried KBr with a weight ratio of 1:10 for all measurements.

Mechanical properties of porous alumina scaffolds obtained by the three synthesis routes (R1, R2, and R3) were estimated through compression tests, where samples were cut to cubic-like blocks, with approximate dimensions of $10 \times 10 \times 10$ mm^3. The surfaces of the samples in contact with the test equipment were infiltrated with acrylic resin, to produce parallel surfaces. Axial compression tests were conducted at 0.5 mm/min using a Universal testing machine (EMIC model DL 3000, max. load 30 kN).

Cytocompatibility, cell viability, and bioactivity assays on porous alumina scaffolds

Vero cells viability was evaluated by spreading and attachment assays. Cells were plated at 6×10^4 density in the presence of macroporous alumina scaffold coated with CaP/PVA coating; Cell spreading was assessed by electron microscopy examination of the specimens after culturing for 2 h. For electron microscopy, specimens were fixed with 2% Glutaraldehyde for 16 h and dehydrated by passing through a series of alcohols (ethanol) before they were dried in nitrogen flowing reactor for 4 h and outgassed in vacuum desiccator for 12 h. Samples were coated with a thin layer of sputtered Au to examine the cell morphology using a SEM.

Results

Materials characterization

Alumina powders

Chemical analysis by X-ray fluorescence (XRF) of alumina powder (A-01) has indicated minor content of the elements iron and sulfur, and traces of calcium and phosphorus. Quite similar results of chemical analysis were found for alumina powder (A-02) with the presence of the same minor elements (Fe, S) and traces of chrome and phosphorus (Cr, P).

X-ray diffraction analysis was conducted in order to verify the crystallinity and major phases present in the alumina powders. Alumina powder sample (A-01) from a local supplier was found to be highly crystalline α-alumina phase. On the other hand, for alumina sample (A-02), XRD results have indicated γ-Al_2O_3 as the major crystal phase with estimated equivalent fractions (50%) of γ-alumina crystalline phase and of amorphous phase.

The particle size distribution analysis was done by laser scattering. SEM and BET method were also employed as supporting techniques for powder analysis. During the characterization procedure it was verified that the material A-01 (α-alumina) "as received" was not adequate for the production of a stable and fine particle size suspension due to the broad distribution and large average particle size. Therefore, particle milling was used without optimizing the operational parameter conditions. Nevertheless, a reduction of average particle size was reached by the milling

Table 2 Particle size distribution of alumina powder A-01

Sample A-01	Particle size (μm)
D_{10}	0.2
D_{50}	4.0
D_{90}	9.0
$D_{average}$	4.3

procedure after 48 h. These results are summarized in Table 2. Supplementary particle size evaluation was conducted by SEM and surface area analysis. SEM photomicrographs of alumina sample (A-01) "as received" and after 48 h milling are showed in Figs. 1a and b, respectively. It was obtained alumina particles typically ranging from ~0.5 to 5.0 μm, which were lately used as ceramic powder for suspension preparation (A-01). Also, an increase of about 10–20% on the specific surface area for alumina powder (A-01) after milling was measured by BET nitrogen adsorption method (from ~3.0 to 3.5 $m^2\ g^{-1}$). These results have confirmed the particle size distribution values presented in Table 2 for α-alumina (A-01).

From Laser scattering results, the median particle size (d_{50}) of alumina powder (A-02) was found to be of 2.2 μm. Further characterization though SEM and multipoint BET nitrogen adsorption measurements were conducted and surface area was estimated aiming to evaluate the γ-alumina sample (A-02) regarding to the particle size and morphology. A typical SEM micrograph of γ-alumina powder (as received) is presented in the Fig. 1c. It should be pointed out that even at 10,000× magnification many agglomerates can be observed as well as individual particles in the nanosize order range (Fig. 1d). In addition, a multipoint B.E.T. analysis of γ-alumina powder (as received) has indicated an average surface area of 34–40 $m^2\ g^{-1}$.

Polyurethane template

SEM micrograph of the PU used (Fig. 2) shows that it has a porous interconnected structure with rounded and regular pores varying in size from 200 to 500 μm, and typical wall thickness of 100 μm.

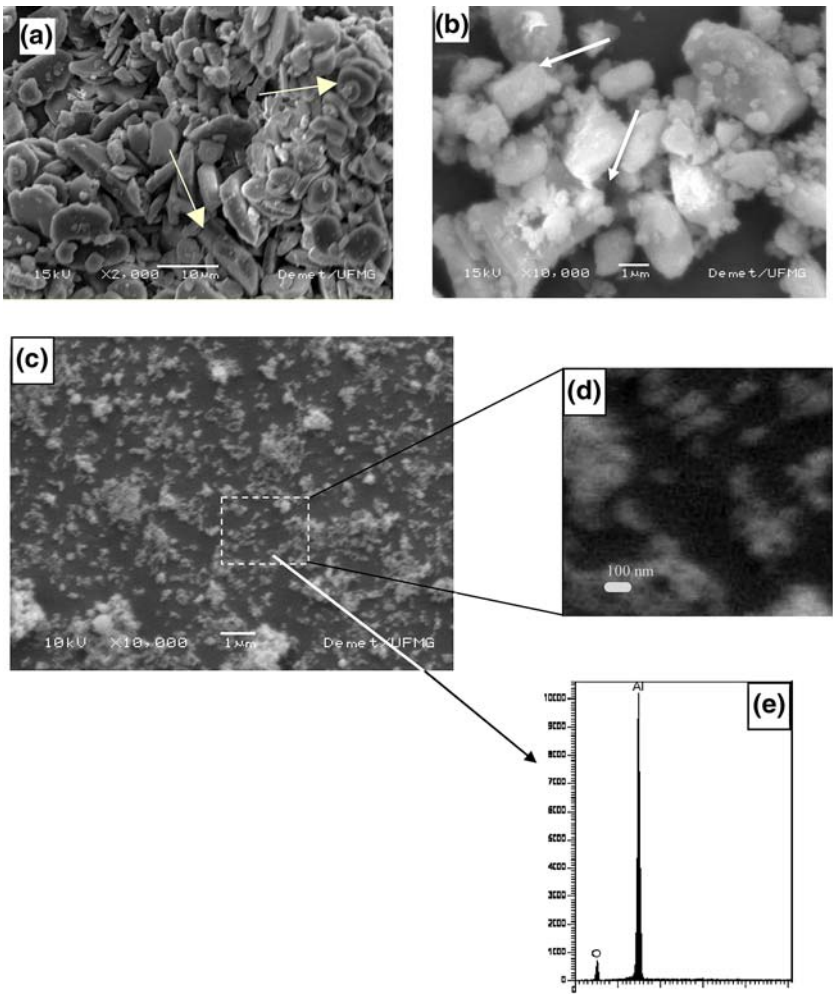

Fig. 1 SEM photomicrographs of alumina A-01 (**a**) as received (2,000×); (**b**) after 48 h milling (10,000×); (**c**) γ-alumina powder (as received, 10,000×); (**d**) Image zoom with γ-alumina (size of ~50 nm); (**e**) EDX spectrum obtained from A-02 sample

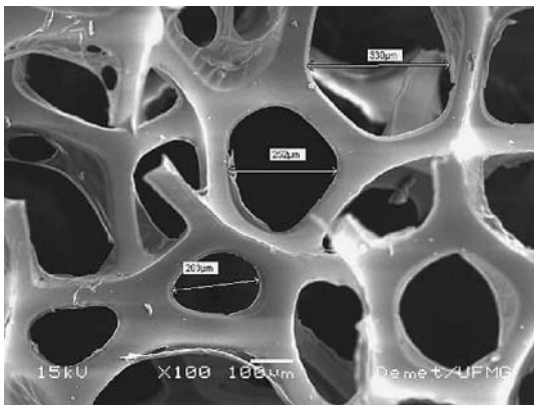

Fig. 2 SEM micrograph of the polyurethane template

Calcium phosphate powder

The calcium phosphate powder used as bioactive coating of alumina scaffold was synthesized via aqueous precipitation route, which has been extensively characterized in previously reported research of group [15]. XRD patterns have indicated a low crystallinity CaP powder, with approximately 80% of amorphous phase and 20% of mostly apatite-like crystalline phases (β-TCP, hydroxyapatite).

Alumina scaffolds production

Preparation of alumina suspensions

In this work, slip casting with low-concentrated alumina slurries were studied as functions of two different dispersants, i.e., poly(acrylic acid) (PAA) and Poly(Vinyl Pyrrolidone) (PVP). Figure 3 illustrates the sedimentation behavior of suspensions prepared using alumina (A-01) with addition of PAA and PAA/PVA. These results showed that the suspensions dispersed with PAA are very stable when compared to the blank sedimentation test without any dispersant added. The pH of the suspension measured after adding PAA was 6.5, compared to pH = 9.5 of the suspension before the additives. The effect of the suspension pH on the PAA adsorption is illustrated in Fig. 4. The decrease of pH and consequent decrease in PVA adsorption may have led to an increase in the concentration of polymer available in the suspension, promoting agglomerate formation and increasing sedimentation (Fig. 5). It was observed that for the suspensions prepared without addition of the dispersant PAA, by adding PVA the sedimentation rate has increased. The final volume of the deposit also increased with the concentration of PVA (Fig. 5).

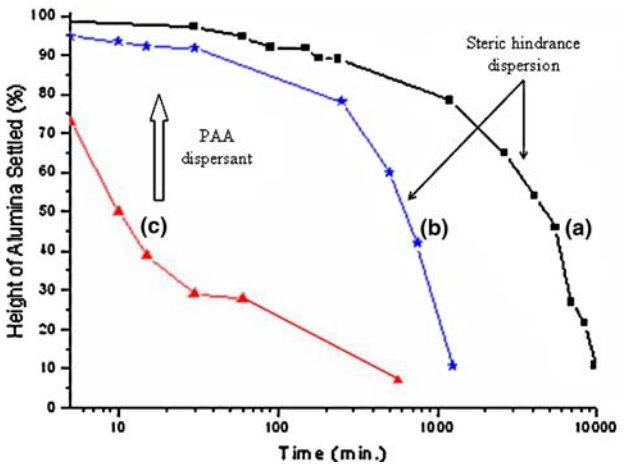

Fig. 3 Effect of PAA and PAA/PVA on the sedimentation behavior of alumina A-01 suspensions. (**a**) Suspension dispersed with 0.3 wt% PAA and pH 6.5; (**b**) suspension dispersed with 0.3 wt% PAA, 0.1 wt% PVA, and pH 6.5; (**c**) suspension prepared without additives and pH 9.5

Polymer foam replication

A procedure used to avoid an excess of suspension in the template pores and to improve replication was a gentle compression of the PU samples with tweezers, to force the suspension out. This procedure has proven to be suitable for leading to a more homogeneous deposition on the pore walls and a better replication of the template. The volume of the suspension deposited on the PU template with only one immersion was not sufficient to completely cover the

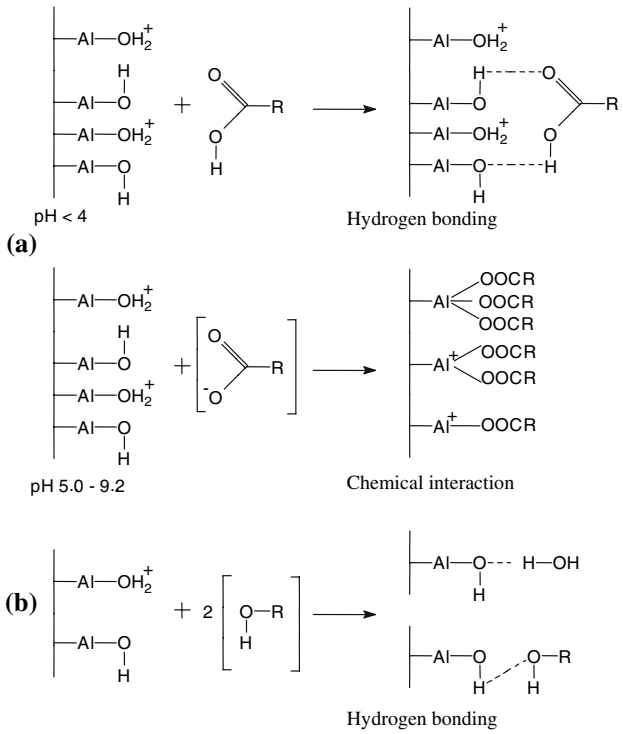

Fig. 4 Schematic representation of the interaction between (**a**) alumina–PAA and (**b**) alumina–PVA (adapted from [16])

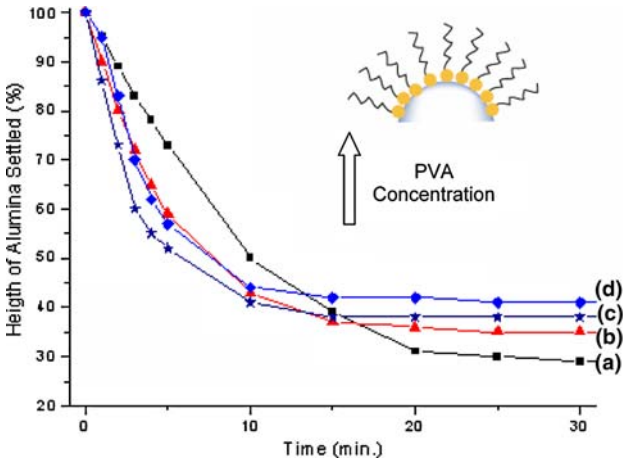

Fig. 5 Effect of PVA concentration on the sedimentation behavior of alumina A-01 suspensions. (**a**) 0.0 wt%; (**b**) 0.4 wt%; (**c**) 0.8 wt%; and (**d**) 1.2 wt%

wall surface. The immersion for three times resulted in a more efficient and complete coverage of the mold. This procedure led to a successful replication, as showed in Fig. 6, and was adopted for all samples in this study.

Figure 7 presents SEM micrographs of the alumina scaffolds obtained with the different suspension preparation routes that have been used. Samples produced by route#1 (R1) (Fig. 7a) presented regions with an excess of ceramic material deposited, which caused the obliteration of some pores, and other regions with less deposited material, leading to fractured and void containing pore walls after sintering. In route#1, the experiment has been carried out by using PVP as a dispersant, with solid concentration showed in Table 1, by adding PVP in mixtures of ethanol (EtOH) and water. Samples produced via route#2 (R2) (Fig. 7b) seem to have less pores obliterated by excess of ceramic material deposited compared so the ones obtained by R1. The best replication was obtained with route R3, as showed by Fig. 7c, in which it can be observed that the deposition was very homogeneous and the pore walls seem to have a larger diameter. The surface of the struts, illustrated for samples obtained by R3 in Fig. 7d, is more dense and smoother than the ones obtained by R1 and R2.

Mechanical behavior of alumina scaffolds

The compressive strength measured for the macroporous alumina scaffolds produced by the three routes used in this work are presented in Table 3. For routes R1 and R2 that used coarser alumina particles (A-01), the measured values for compressive strength were 1.9 and 1.6 MPa, respectively. The compressive strength for samples fabricated with γ-alumina samples (A-02) was 3.3 MPa.

Alumina scaffolds coating

XRD analysis of porous samples submitted to the biomimetic coating procedure, either before and after immersion

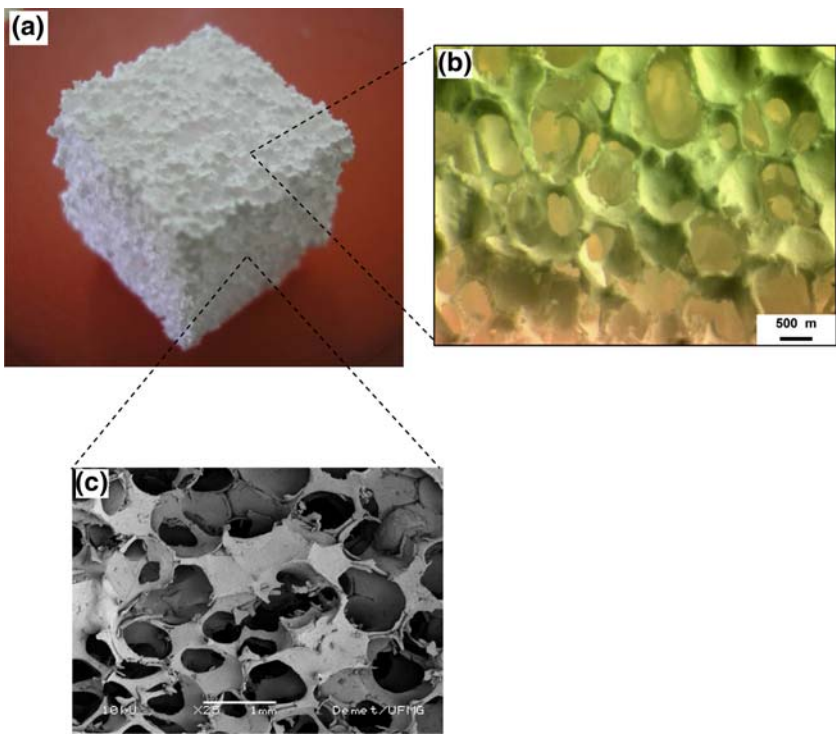

Fig. 6 Optical micrograph of alumina scaffolds produced showing the appropriate replication obtained with the immersion procedure used

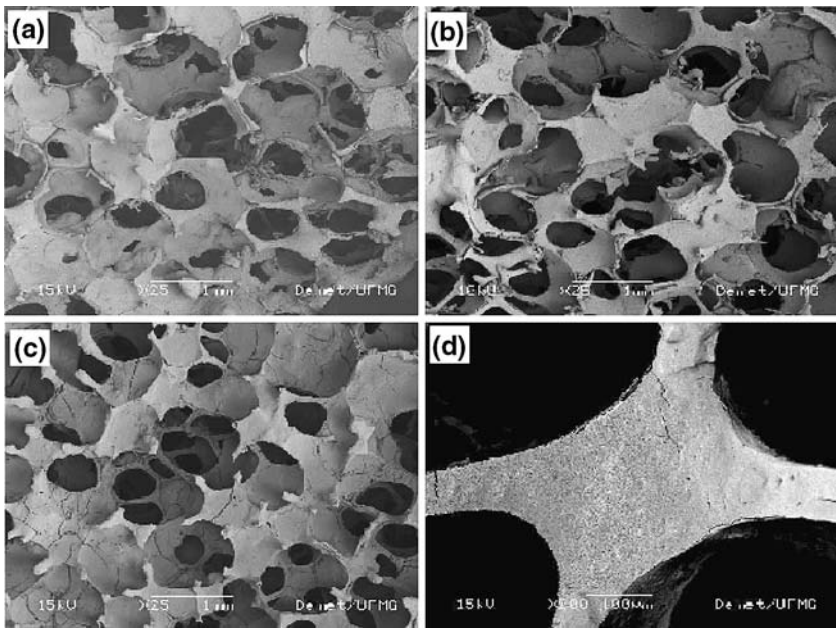

Fig. 7 SEM micrographs of the alumina scaffolds obtained. (**a**, **d**) Route R1; (**b**) Route R2; and (**c**) Route R3

Table 3 Compressive strength measured for the alumina scaffolds produced by different routes

Route	Compressive strength (MPa)
R1	1.9
R2	1.6
R3	3.3 ± 1.0

in the zinc (Zn^{2+}) containing solution, showed peaks characteristic only of α-alumina phase characteristic of the porous substrate. There was no indication of the presence of a calcium phosphate phase or of a zinc-containing phase. EDX analysis confirmed the presence aluminum oxide, but no other element present on the surface. These results show that there was no detectable deposition of a calcium phosphate layer on the surface of the scaffolds when the biomimetic procedure was used.

Calcium phosphate/PVA slurry was used as the second coating method for alumina scaffolds. It was clearly observed that a calcium phosphate coating was deposited onto the scaffold pore walls. In Fig. 8, it is showed a sequence of SEM micrographs of a sample coated by immersion in the CaP/PVA suspension. Open pores with diameters in the range from 150 to 800 μm were clearly observed. It was also apparent that some obstruction of pores has occurred, maybe due to an excess material transferred. EDX analysis on the coated samples showed the presence of Al, Ca, and P peaks, indicating that the calcium phosphate layer was successfully deposited onto the alumina porous structure.

The incorporation of the zinc divalent ion (Zn^{2+}) was conducted by soaking the alumina scaffold coated with CaP layer in $Zn(NO_3)_2$ aqueous/ethanol solution. During immersion of the coated samples in the solution (Zn^{2+}), cloudiness of the solution occurred, suggesting that part of the coating was removed. This fact was confirmed by SEM micrographs (Figs. 8b and d), which showed that the porosity increased and the thickness of the CaP layer has decreased. The average thickness of the CaP/PVA coatings varied between 20 and 30 μm. CaP coatings with zinc incorporated have presented an estimated thickness of 9–15 μm and were more homogeneous and regular (Fig. 8e and f) than without Zn^{2+}. EDX analysis has confirmed the incorporation of Zn^{2+} in the CaP layer after the immersion in the solution.

XRD analysis of the CaP/PVA coated scaffolds, with and without Zn^{2+} incorporation, showed peaks corresponding to the α-alumina phase of the scaffold, as illustrated in Fig. 9. In addition, the detailed insert in Fig. 9 showed a small peak at 32° corresponding to regions of the more intense peaks for PVA and calcium phosphate, which confirmed the presence of the calcium phosphate layer. The identification of the calcium phosphate layer was also verified by FTIR analysis, as showed in Fig. 10. Bands corresponding to the vibration modes of νPO_4^- group (565, 599, 960, and 1041 cm^{-1}) and to νCO_3 group (871, 1414, and 1454 cm^{-1}).

Cytocompatibility and bioactivity assays on porous alumina scaffolds

VERO cell spreading and adhesion test on the developed alumina scaffolds was used as the evaluation of the cytotoxicity and biocompatibility of samples. Cell spreading was primarily assessed by SEM examination of the specimens.

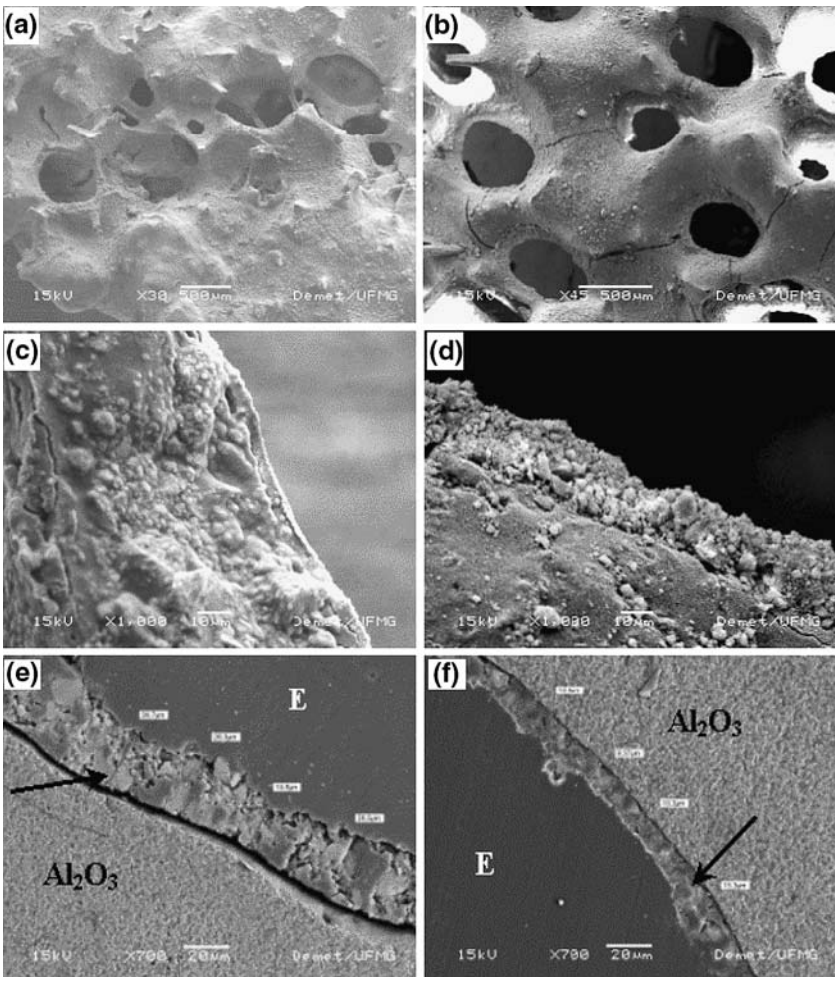

Fig. 8 SEM micrographs of porous alumina scaffolds coated in a CaP/PVA suspension before (**a**, **c**, **e**) and after immersion in zinc containing solution (**b**, **d**, **f**). The magnifications (**c** and **d**) show the pore wall with the deposited layer. Transversal sections of embedded samples allow better visualization of the CaP/PVA coatings

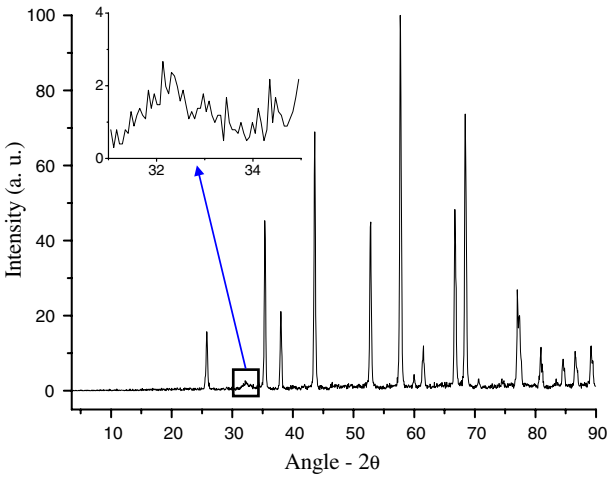

Fig. 9 XRD diffraction pattern of porous alumina scaffold coated with a CaP/PVA layer and incorporated with zinc

As showed in Fig. 11a and b, cells spreading and attachment were clearly verified on alumina macroporous structured samples coated with CaP layer.

Discussion

Materials characterization

Alumina powders

The alumina powders characterization procedure was conducted in order to evaluate their chemical composition, crystallinity, particle size distribution, and particle morphology. Regarding to chemical XRF results no significant contamination was found in both alumina samples (A-01 and A-02) analyzed.

X-ray diffraction patterns have showed that alumina powder from a local supplier (A-01) was found to be highly crystalline based on α-alumina phase. In contrast, alumina sample (A-02) has indicated to be partially amorphous (~50%) and partially γ-Al_2O_3 crystalline phase according to the ICDD card no. 10-0425. That was by some means expected based on the process used for high purity and nanosized alumina particles, generally through sol-gel process using hydrolysis of aluminum alcoxides. This

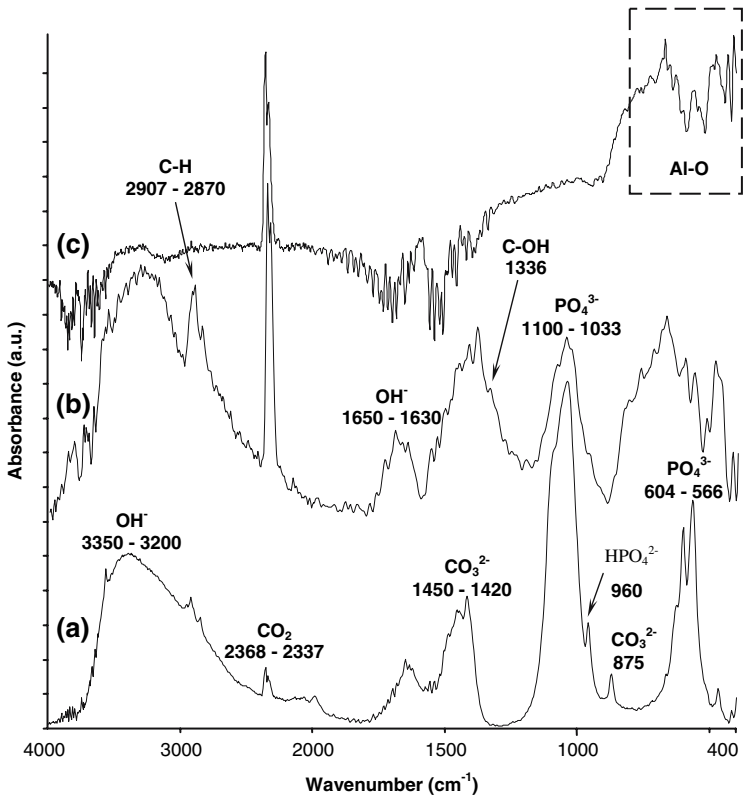

Fig. 10 FTIR diffuse reflection spectra of CaP and alumina powders (**a** and **c**) and of the alumina scaffolds coated with CaP/PVA

aqueous chemical route usually produces some hydroxides and amorphous phases [17].

A-01 (α-alumina) "as received" was found to be inappropriate for suspension preparation due to its coarseness and broad particle distribution. Therefore, a milling procedure would be needed in order to get a finer and tighter particle size distribution, reaching for the production of a more stable ceramic suspension. In fact, the objective was achieved after 48 h milling as results presented in Table 2. These results were endorsed by both SEM and BET surface analyses. SEM micrographs of alumina sample (A-01) "as received" and after 48 h milling are showed in Fig. 1a and b, respectively. It can be noted that qualitatively the particle after milling are slightly smaller that that as supplied. In addition, BET results have showed evidence that an increase of surface area estimated to be about 10–20% on the alumina powder (A-01) after milling was measured by BET nitrogen adsorption method (from ~3.0 to 3.5 $m^2\ g^{-1}$). In summary, it may be said that the milling method has been effective on reduction the average alumina particle size, which is crucial for stabilizing ceramic powder suspension.

It must be stated that the main reasons leading to the selection of γ-alumina nanosized powders were: (i) the highest purity and quality available on the market to be compared to local supplier; (ii) alumina particles in the nanosize (or nanometric) range for slip casting of macroporous tri-dimensional interconnected structure. Based on that, according to the literature the smallest α-alumina powder that is commercially available has median particle size of approximately 0.2 μm [12]. That means, α-alumina was not in readily available with particle size under 200 nm. Therefore, the choice for a nanosized alumina was made (Catalog #544833, Aldrich). However, from Laser scattering results, the median particle size (d_{50}) of alumina powder (A-02) was found to be of 2.2 μm. Such value was not in agreement with the technical data sheet from supplier. Besides that, it was referenced as nanosized particles in the range of 40–47 nm, quite far from the valued obtained via laser scattering. Therefore, further characterization was needed to investigate the actual particle size and morphology claimed by the manufacturer. Hence, SEM and multipoint BET nitrogen adsorption measurements were conducted and surface area was estimated. It was confirmed by SEM results (Fig. 1c) that at 10,000× magnification many agglomerates were clearly observed as well as individual particles in the nanosize order range (Fig. 1d). In addition, a multipoint B.E.T. analysis of γ-alumina powder (as received) has indicated an average surface area of 34–40 $m^2\ g^{-1}$ in agreement with surface area of 35–43 m^2/g reported in the supplier technical catalog (Catalog #544833, Aldrich). As a consequence, that result has confirmed the surface area value indicated by the manufacturer. In addition to that, the specific surface area found in our work has given strong evidence that despite of some agglomerates observed in the

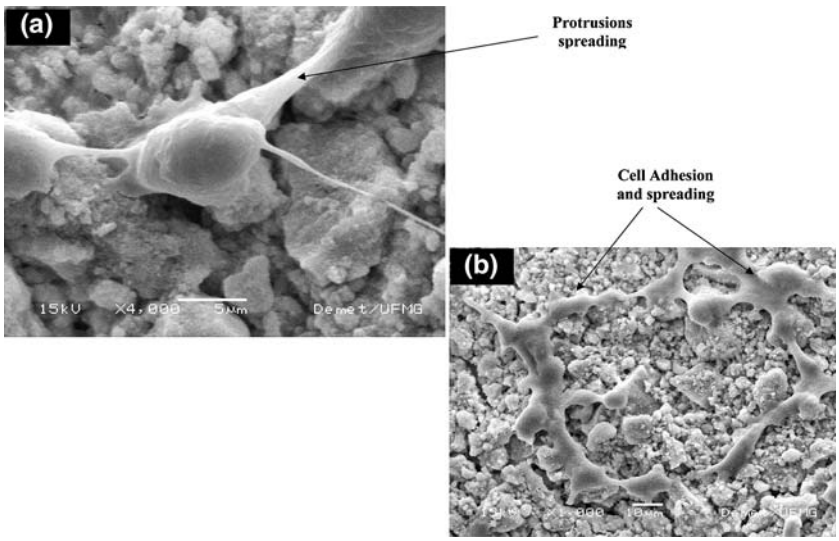

Fig. 11 VERO cells spreading and attachment assays. SEM photomicrograph of cell spreading and adhesion on alumina macroporous structured samples coated with CaP layer (**a** and **b**)

SEM micrographs, the γ-alumina powder is truly in the nanosize range of particle size distribution. In summary, from the results it is reasonable to assume that due to the presence of agglomerates, the particle size distribution obtained by laser scattering was inaccurate and "shifted" to higher median size and not corresponding to the actual particle size as verified by complementary analysis techniques and endorsed by the supplier (40–47 nm).

Polyurethane template

The morphology of the struts of polyurethane (PU, 50 ppi) used as template had a decisive role in the final structure of the 3D porous ceramic obtained. SEM micrograph of the PU have indicated a porous interconnected structure with pores ranging typically from 200 to 500 μm, and typical wall thickness of 100 μm. Therefore, it is suitable for hosting bone cells (~150–300 μm) colonization allowing the future the in-growth of bone tissue to achieve full integration with the living bones [9].

Alumina scaffolds production

Preparation of alumina suspensions

Slip casting is one of the most common forming techniques used in the fabrication of ceramics. To obtain successful casting results, one needs first to fully deagglomerate the ceramic powders and get concentrated slurries with good rheological properties [18]. In the present study, two dispersants were investigated. Poly (acrylic acid) or PAA was chosen as dispersant because it has a strong interaction with the surface of alumina particles due to the carboxylic group. Generally, the PAA carboxylic group can act as proton donor or receptor, leading to adsorption by hydrogen bonding with the hydrolyzed alumina surface [19]. Poly (vinyl pyrrolidone) or PVP has been reported as an effective dispersant on polar and non-polar solvent interaction of ceramic slurries [20].

The sedimentation behavior of suspensions prepared using alumina (A-01) with addition of PAA and PAA/PVA were investigated (Fig. 3). These results showed that the suspensions dispersed with PAA are very stable, in accordance with results obtained by Palmquist and co-workers [21]. The observed stability shows that the polymer is adsorbed efficiently at the alumina particle surface when compared to the blank sedimentation test without any dispersant added. Apparently the addition of PVA to the suspension dispersed with PAA decreases the stability, increasing the sedimentation rate. The effect of the simultaneous addition of PAA and PVA at low pH values has been discussed in the literature [16] by suggesting that the reduction on PVA adsorption was related to the decrease of available sites on the surface of alumina and also to the formation of hydrogen bonding inter and intra-chains of polymers. As expected, the addition of a PAA (acid) has significantly altered the pH of the alumina suspension from pH = 9.5 to 6.5. The concentration of non-adsorbing free polymer is effectively reduced between the particles, and the higher concentration outside the particle–particle approach zone, exert an osmotic pressure causing the particles to flocculate [22]. As certainly expected, both suspensions containing PAA and PAA/PVA were more stable than the suspension without additives. The interaction of various polyalcohol binders with fine, high-purity alumina powder was investigated by some authors [23]. It is important to mention that the vinyl alcohol functionality found in polyvinyl alcohol (PVA), poly(vinyl butyral), and partially hydrolyzed polyvinyl acetate (PVAc) are known to be responsible for a number

of important adsorption and binding mechanism to surfaces. In other words, the degree of hydrolysis of PVA may be to some extent responsible for balance of charges and H^+ interaction at the interface polymer–alumina particle surface.

When the suspensions were prepared with γ-alumina A-02, even without additives, the stability of the suspensions was much higher than the observed for suspensions prepared with A-01. Such effect was likely to be observed due to the nanosize particle distribution and very high surface area of alumina sample A-02 (~30 m^2 g^{-1}) about 10 times higher compared to alumina sample A-01 (~3 m^2 g^{-1}). Also, the presence of negatively charged aluminol groups on its surface may cause repulsion and, hence acting to some extent as dispersant. In A-02 suspensions, where the particle size is much finer, the high molecular weight of PAA molecule used in the experiments has a superior relative size compared to the other system (A-01), causing a different behavior with the formation of "bridges" between alumina particles, which facilitates the formation of aggregates and increases the viscosity [24]. Based on these results, it was established that A-02 suspensions would be prepared with no addition of PAA but a low content of PVP dispersant instead.

Polymer foam replication

The synthesis via route#1 (R1) with the coarser alumina powder A-01 (d_{50} = 4.2 μm) and with the addition of PVP resulted in suspensions not efficiently dispersed and with many agglomerates were formed. As a result, the structures have presented a rough surface and microporosity on the pore walls of struts. The addition of PAA (R2) increased the dispersion and fluidity of these suspensions. In fact, PAA is well known as a polymer able to act as dispersant with expressive adsorption at the alumina surface, and may enhance the adsorption of PVP [16, 25]. Hence, suspensions formed via route#2 (R2) showed higher fluidity and produced porous scaffolds with walls more densely packed and smoother than R1. In addition, pore walls of alumina scaffolds seemed to be narrower than those ones obtained when suspensions were not prepared with PAA.

In the case of scaffolds produced using alumina A-02, with nanosized particles and high-specific surface area, the suspensions were dispersed by PVP without adding PAA. Highly dispersed and fluid suspensions were efficiently deposited on the walls of PU template, with a superior amount transferred than samples produced with alumina A-01. Besides the higher efficiency of deposition of the suspension, the use of a fine particle size distribution alumina increases densification and decreases the final grain size [26]. In agreement to that, the scaffolds obtained through route (R3) using A-02 nanometric particles have presented denser and smoother pore walls than it was observed for A-01 alumina samples.

Our results also indicated that an adequate coverage of polyurethane replica was obtained when using ethanol/water mix as solvent. Such behavior is thought to be related to the interactions that have taken place in the complex system based on polyurethane-dispersant–alumina-solvent. The balance of electrostatic forces of water and dispersant adsorbed onto alumina surface with van der Waals and hydrophobic forces associated with polyurethane polymer template used a template to be uniformly and evenly coated. Ethanol (EtOH) added to the suspension would play an important role as a less polar solvent, like reported in several papers in the literature of alumina suspensions with non-polar solvents [9, 20].

The scaffold structures obtained in this study, with pore size ranging from 100 to 300 μm and high-interconnected porosity, is potentially effective to allow tissue ingrowth in implant devices and consequently a mechanism of prosthesis fixation in the host tissue, as well as vascularization and blood supply.

Mechanical behavior of alumina scaffolds

Concerning to the mechanical properties, the results were based on the compressive strength behavior measured for the macroporous alumina scaffolds produced by the three routes used in this work. Although samples produced by R1 presented a rougher surface and presence of microporosity on the walls of struts, due to a less efficient dispersion, a larger deposited volume and consequent thicker pore walls, may account for the higher value observed in relation to samples obtained by R2. The average compressive strength for samples produced via route#3 with γ-alumina samples (A-02) was 3.3 MPa. As expected, these results show a significant increase in the strength of samples produced with finer and well-dispersed particles. Compressive strength of bioceramic porous scaffolds have been reported in the literature, such as hydroxyapatite (HA) scaffolds [27–30] varied from 0.3 to 5.0 MPa, depending on the solids contents in the HA suspension and porosity. The compressive strength of tri-dimensional macroporous alumina scaffolds obtained in this work using route R3 is in the same level as some published results for ceramic based macroporous scaffolds, and significantly higher than others [9, 31]. It should be pointed out that these values are very much depended on several process parameters such as particle size and distribution, solid content on the suspension, additives and surfactants, temperature and so forth. Also, not only the total porosity but also the interconnectivity will have a significant role on the mechanical behavior of these highly porous materials structures. In fact, the compressive strength should be analyzed in

conjunction with true density and porosity at macro, micro, and nanostructure level. The major application for the developed alumina macroporous structure is related to the replacement of small lesions on bone tissue, for instance the trabecular (cancellous) bone due its highly porous structure. Different bone tissues differ in their amounts of porosity, mineralization, reconstruction, and preferred orientation. All these have important effects on mechanical properties. Very porous, trabecular bone is always weaker and more compliant than compact bone on a weight for weight basis, yet it occurs in places where its energy absorbing ability, or its low density, is advantageous. As a reference, considering donor age, gender, among several other factors the range expected for ultimate stress bone from 2 to 10 MPa in trabecular bone when evaluated by compressive mechanical test. The results related to mechanical properties of the alumina porous scaffolds presented in this work were found to be in the suitable range for trabecular bone tissue substitute [32–34].

Alumina scaffolds coating

Alumina has long been known as a bioinert material as far as replacement of bone tissue is concerned. On the other hand, the high mechanical properties of alumina-based ceramics have driven many researchers to combine with more biocompatible materials for instance, calcium phosphates [35]. As a consequence, in the present study two different coating methods were evaluated in order to have a bioactive layer deposited on macroporous alumina scaffolds: (a) biomimetic and (b) immersion in calcium phosphate/PVA slurry. The biomimetic process is based on a deposition of a thin CaP layer on the surface of the material by immersion in a protein-free acellular simulated body fluid (SBF or Kokubo's solution) where ion exchange takes place. However, based on the SEM/EDX, XRD, and FTIR results, no detectable calcium phosphate layer was found on alumina scaffold samples submitted to the biomimetic method. The absence of precipitation of a CaP layer on the alumina scaffold by the biomimetic method may be explained by the fact that SBF solution has pH = 7.4, at which the alumina surface is positively charged. Several reports in the literature have indicated that heterogeneous CaP precipitation is generally associated with negatively charged surfaces, such as silica and titania [36–39] or other negatively charged materials such as cellulose beads [40] and collagen [41]. A negative surface charge at neutral pH values leads to the formation of an electrical double layer with an increased concentration of cations at the interface. The concept of the electrical double layer was applied to the analysis of HA precipitation on negative silica glass surfaces [42]. The consequent increase at the concentration of cations at the interface then guided to the nucleation of HA. In the sequence, the research was later extended by studying the precipitation of HA on three different oxides, silica, titania and alumina, immersed in SBF solution [43]. They showed that HA precipitation occurred on silica and titania substrates, both presenting negative surface charges at physiological solution pH, but HA precipitation did not occur on alumina, which presents a positive surface charge. As a result, in the present work, precipitation of CaP on the alumina surface did not occur even from a supersaturated solution (1.4SBF). In the SEM analysis it was observed that the surface presented a more irregular topography compared to the control samples immersed in deionized water, indicating that the α-alumina matrix may have partially reacted during the immersion in SBF solution. Nonetheless, similar to other oxide solid substrates with high-specific surface area, many broken bonds are present at the surface (aluminol groups) which may cause some degradation related to ionic interaction and partially water soluble hydroxides are formed. As reported in the literature, it appears that alumina due mainly to its high-specific surface area and to the presence of aluminol groups on its surface is progressively transformed to hydroxides [36].

The second deposition method used to produce a biocompatible layer onto synthesized macroporous alumina tri-dimensional structures was based on the immersion in a calcium phosphate and PVA suspension. The deposition method was effective on producing a CaP/PVA coating on the alumina samples, as it was evidenced by results from SEM and EDX. Also, FTIR spectroscopy results have endorsed the formation of the calcium phosphate layer, as showed in Fig. 10. Bands corresponding to the vibration modes of νPO_4^- group (565, 599, 960, and 1041 cm^{-1}) and to νCO_3 group (871, 1414, and 1454 cm^{-1}), characteristic of the apatites, are present (Fig. 11b) [14]. In these spectra bands corresponding to the C–OH group at 1336 cm^{-1} of PVA, and bands corresponding to the Al–O bond in the region below 700 cm^{-1} are also present [44, 45].

Of the many trace elements, Zinc (Zn^{2+}) is naturally present in bone and stimulates bone growth and biomineralization. Zinc ions are also known to modify the production of cytokines and increases bone protein. Furthermore, it has been reported that divalent zinc cations associated with calcium phosphates has enhanced the bioactivity in bone tissue regeneration. It should be mentioned that zinc must be released slowly from the implant because zinc at an elevated level induces adverse reactions [13]. Therefore, the incorporation of the zinc divalent ion (Zn^{2+}) was conducted by soaking the alumina scaffold coated with CaP layer in $Zn(NO_3)_2$ aqueous/ethanol solution. Based on the SEM/EDX micrographs and chemical analysis, it was clearly verified that CaP coatings with zinc incorporated were deposited on the alumina 3D scaffold. Also, XRD data have confirmed the presence of Zn^{2+} phase in the CaP

layer. Due to very low wavenumber associated with metal oxides such as ZnO, CaO (<400 cm^{-1}) no vibrational bands were identified by FTIR analysis that might be related to the presence of zinc incorporated in the CaP coatings. In summary, it was demonstrated that the CaP/PVA suspension deposition procedure was able to create a calcium phosphate coating onto the surface of the macroporous alumina scaffolds, with or without zinc cation incorporated, which may act as a bioactive layer. These findings are quite relevant once it has been recently [11] demonstrated that using Zn^{2+} associated with calcium phosphates has enhanced the bioactivity in bone tissue regeneration. It should be pointed out that the coating procedure has to be optimized, aiming to achieve a more uniform calcium phosphate coating yet without decreasing the scaffold porosity by blocking some pores of the tri-dimensional alumina scaffold. Regarding to mechanical properties, evaluated through uniaxial compressive tests, no significant statistical difference was observed between alumina bodies coated and uncoated with calcium phosphate/PVA. That would be by some means expected based upon the well-known small influence of CaP surface coatings on the overall compressive strength and compressive modulus of alumina ceramics [9].

Cytocompatibility and bioactivity assays on porous alumina scaffolds

Safety tests including cytotoxicity assays are required for all products to be used in contact with human beings. Cytotoxicity tests using cell cultures have been accepted as the first step in identifying active compounds and for biosafety testing. Cell adhesion is involved in various natural phenomena such as embryogenesis, maintenance of tissue structure, wound healing, immune response, metastasis, and tissue integration of biomaterials [46]. Since cellular attachment, adhesion, and spreading belong to the first phase of cell/material interactions, the quality of this phase will influence proliferation and differentiation of cells on biomaterials surfaces. Based on the SEM results obtained in our work, one may attribute the VERO cell spreading and adhesion verified on the 3D alumina scaffolds coated with CaP layer to be a reliable proof of biocompatibility and no cytotoxicity of samples. According to the literature [46–48], cell spreading are usually divided into three main interaction levels: (a) not spread: cells were still spherical in appearance, protrusions or lamellipodia were not yet produced; (b) partially spread: at this stage, cells began to spread laterally at one or more sides, but the extensions of plasma membrane were not completely confluent; and (c) fully spread. The last model (c) would represent the best result for material cell hosting. Based on that, the 3D macroporous alumina scaffold samples with CaP coating produced in this study has proven to be biocompatible and with elevated potential for cell culture and growth.

Conclusions

Well-dispersed and fine particle size suspensions led to a successful replication and production of alumina scaffolds, with high-interconnected porosity. The compressive strength of alumina scaffolds obtained in present work through route R3 was found to be in the suitable range of mechanical properties for trabecular bone tissue substitute. In addition to that, a calcium phosphate coating was successfully deposited onto the tri-dimensional porous alumina scaffold by using CaP/PVA slurry. The CaP layer was later chemically modified with the incorporation of Zn^{2+}. Cells viability, proliferation, and also material cytotoxicity were verified by cell spreading and attachment assays on the alumina porous scaffold coated with PVA-calcium phosphate. In summary, a new process was developed to obtain alumina with tri-dimensional porous structure and covered with a biocompatible coating of calcium phosphate doped with zinc. Such system has high potential to be used in bone tissue engineering.

Acknowledgments The authors acknowledge CNPq/FAPEMIG/CAPES for financial support on this project. We are also grateful to Prof Dr Wander L. Vasconcelos for the FTIR spectroscopy facilities and to Prof Dr Dagoberto B. Santos for the SEM Laboratory.

References

1. Kim HM (2003) Curr Opin Solid State Mater Sci 7:289
2. Nissan BB (2003) Curr Opin Solid State Sci 7:283
3. Burg KJL, Porter S, Kellam JF (2000) Biomaterials 21:2347
4. Karageorgiou V, Kaplan D (2005) Biomaterials 26:5474
5. Pereira MM, Jones JR, Hench LL (2005) Adv Appl Ceram 104:35
6. Sá MCC, Moraes B, Elias CN, Filho JD, Oliveira LG (2004) Mater Res 7:643
7. Rezwan K, Chen QZ, Blaker JJ, Boccaccini AB (2006) Biomaterials 27:3413
8. Yeong WY, Chua CK, Leong KF, Chandrasekaran M (2004) Trends Biotechnol 22:643
9. Jun YK, Kim WH, Kweon OK, Hong SH (2003) Biomaterials 24:3731
10. Shi D, Jiang G (1998) Mater Sci Eng C 6:175
11. Grandjean-Laquerriere A, Laquerriere P, Jallot E, Nedelec JM, Guenounou M, Laurent-Maquin D, Phillips TM (2006) Biomaterials 27:3195
12. Han KR, Lim CS, Hong MJ, Jang JW, Hong KS (2000) J Am Ceram Soc 83:750
13. Ramesh S, Sominska E, Cina B, Chaim R, Gedanken A (2000) J Am Ceram Soc 83:89
14. Oliveira M (2004) Synthesis and characterization of bioceramics based in calcium phosphate. MSC Dissertation, Department of Metallurgical and Materials Engineering, Federal University of Minas Gerais, Brazil, 118 p

15. Santos MH, Oliveira M, Souza LPF, Mansur HS, Vasconcelos wl (2004) Mater Res 7:625
16. Santhiya D, Subramanian S, Natarajan KA, Malghan SG (1999) J Colloid Interf Sci 216:143
17. Santos PS, Santos HS, Toledo SP (2000) Mater Res 3:104
18. Tsetsekov A, Agrafiotis C, Milias J (2001) J Euro Ceram Soc 21:363
19. Kasprzyk-Hordern B (2004) Adv Colloid Interf Sci 110:19
20. Zhang J, Jiang D, Lin Q (2005) J Am Ceram Soc 88:1054
21. Palmqvist L, Lyckfeldt O, Carlström E, Davoust P, Kauppi A, Holmberg GK (2006) Colloids Surface A Physicochem Eng Aspect 274:100
22. Khan AU, Briscoe J, Luckham PF (200) Colloids Surfaces A Physicochem Eng Aspect 161:43
23. Khan AU, Briscoe BJ, Luckham PF (2000) Colloids Surfaces A Physicochem Eng Aspect 161:243
24. Yokosawa MM, Pandolfelli VC, Frollini E (2002) J Dispersion Sci Technol 23:827
25. Ishiduki K, Esumi K (1997) J Colloid Interf Sci 185:274
26. Bowen P, Carry C, Luxembourg D, Hofmann H (2005) Powder Technol 157:100
27. Kwon SH, Jun YK, Hong SH, Lee IS, Kim HE, Kwon SH (2002) J Am Ceram Soc 85:3129
28. Le Huec JC, Schaeverbeke T, Clement D, Faber J, Le Rebeller A (1995) Biomaterials 16:113
29. Ramay HR, Zhang M (2003) Biomaterials 24:3293
30. Chang BS, Lee CK, Hong KS, Youn HJ, Ryu HS, Chung SS, Park KW (2000) Biomaterials 21:1291
31. Studart AR, Gonzenbach UT, Tervoort E, Gauckler LJ (2006) J Am Ceram Soc 89:1771
32. Currey J (1984) J Integrat Comp Biol 24:5
33. Anderson MJ, Keyak JH, Skinner HB (1992) J Bone Joint Surg Am 74:747
34. Ding M, Dalstra M, Danielsen CC, Kabel J, Hvid I, Linde F (1997) J Bone Joint Surg 79-b:995
35. Rambo CR, Müller FA, Müller L, Sieber H, Hofmann I, Greil P (2006) Mater Sci Eng C 26:92
36. Song MG, Lee J, Lee Y, Koo J (2006) J Colloid Interf Sci 300:603
37. Li P, Ohtsuki C, Kokubo T, Nakanish K, Soga N, Nakamura T, Yamamuro T (1992) J Am Ceram Soc 75:2094
38. Li P, Groot K (1993) J Biomed Mater Res 27:1495
39. Pereira MM, Hench LL (1996) J Sol-Gel Sci Technol 7:59
40. Krukowski M, Shively RA, Osbody P, Eppley BL (1990) J Oral Maxillofacial Surg 48:468
41. Banks E, Nakajima S, Shapiro LC, Tilevitz O, Alonzo JR, Chianelli C (1977) Science 198:1164
42. Li P, Zhang F (1990) J Non-Cryst Solids 119:112
43. Li P, Ohtsuki C, Kokubo T, Nakanish K, Soga N, Groot K (1994) J Biomed Mater Res 28:7
44. Mansur HS, Oréfice RL, Mansur AAP (2004) Polymer 45:7193
45. Liu J, Jean J, Li C (2006) J Am Ceram Soc 89:882
46. Dunn GA, Zicha D (1995) J Cell Sci 108:1239
47. Bose S, Darsell J, Hosick HL, Yang L, Sarkar DK, Bandyopadhyay A (2002) J Mater Sci Mater Med 13:23
48. Hannah S, Samuel SI (2005) Biomaterials 26:5492